Contributions to Mineralogy and Petrology (2019) 174:20
https://doi.org/10.1007/s00410-019-1554-x

ORIGINAL PAPER

Building Mesoarchaean crust upon Eoarchaean roots: the Akia Terrane, West Greenland

N. J. Gardiner[1,2,3,4] · C. L. Kirkland[1,2,3] · J. Hollis[5] · K. Szilas[6] · A. Steenfelt[7] · C. Yakymchuk[8] · H. Heide-Jørgensen[5]

Received: 1 October 2018 / Accepted: 6 February 2019 / Published online: 26 February 2019

Abstract

Constraining the source, genesis, and evolution of Archaean felsic crust is key to understanding the growth and stabilization of cratons. The Akia Terrane, part of the North Atlantic Craton, West Greenland, is comprised of Meso-to-Neoarchaean orthogneiss, with associated supracrustal rocks. We report zircon U–Pb and Lu–Hf isotope data, and whole-rock geochemistry, from samples of gneiss and supracrustals from the northern Akia Terrane, including from the Finnefjeld Orthogneiss Complex, which has recently been interpreted as an impact structure. Isotope data record two major episodes of continental crust production at ca. 3.2 and 3.0 Ga. Minor ca. 2.7 and 2.5 Ga magmatic events have more evolved εHf, interpreted as reworking of existing crust perhaps linked to terrane assembly. Felsic rocks from the Finnefjeld Orthogneiss Complex were derived from the same source at the same time as the surrounding tonalites, but from shallower melting, requiring any bolide-driven melting event to have occurred almost simultaneously alongside the production of the surrounding crust. A simpler alternative has the Finnefjeld Complex and surrounding tonalite representing the coeval genesis of evolved crust over a substantial lithospheric depth. Hafnium isotope data from the two major Mesoarchaean crust-forming episodes record a contribution from older mafic Eoarchaean crust. Invoking the involvement of an Eoarchaean root in the growth of younger Mesoarchaean crust puts important constraints on geodynamic models of the formation of the discrete terranes that ultimately assembled to form Earth's cratons.

Keywords Archean · TTG · North Atlantic Craton · Hf isotope evolution · Partial melting anatexis

Introduction

Up to 75% of Earth's continental crust may have had its genesis during the Archaean Eon (4.0–2.5 Ga) (Belousova et al. 2010; Dhuime et al. 2012; Hawkesworth et al. 2017). This early felsic crust is largely comprised of

Communicated by Othmar Müntener.

Electronic supplementary material The online version of this article (https://doi.org/10.1007/s00410-019-1554-x) contains supplementary material, which is available to authorized users.

✉ N. J. Gardiner
nick.gardiner@monash.edu

[1] Centre for Exploration Targeting, Curtin Node, School of Earth and Planetary Sciences, Curtin University, Perth, Australia

[2] The Institute for Geoscience Research (TIGeR), School of Earth and Planetary Sciences, Curtin University, Perth, Australia

[3] Australian Research Council Centre of Excellence for Core to Crust Fluid Systems, Perth, Australia

[4] Present Address: School of Earth, Atmosphere and Environment, Monash University, Melbourne, VIC 3800, Australia

[5] Department of Geology, Ministry of Mineral Resources, Government of Greenland, P.O. Box 930, 3900 Nuuk, Greenland

[6] Department of Geosciences and Natural Resource Management, University of Copenhagen, Øster Voldgade 10, 1350 Copenhagen K, Denmark

[7] The Geological Survey of Denmark and Greenland, Øster Voldgade 10, 1350 Copenhagen K, Denmark

[8] Department of Earth and Environmental Sciences, University of Waterloo, Waterloo, ON N2L 3G1, Canada

composite gneisses, volumetrically dominated by rocks of the tonalite–trondhjemite–granodiorite (TTG) series (Moyen 2011 and refs therein). Constraining the nature of Archaean felsic crust production, including: source, geodynamic setting, rate of production and volumetric extent, temporal melting patterns, and geochemical evolution, is key to understanding the inception and development of Earth's continental nuclei—the Archaean cratons. Most exposed Archaean cratons are, however, dominated by low-grade granite–greenstone associations, hindering study of their high-grade gneissic cores. In contrast, the North Atlantic Craton (NAC), cropping out in Labrador, southern West Greenland, eastern Greenland, and northwestern Scotland, is mainly comprised of well-exposed Eo-to-Neoarchaean TTG orthogneisses, with supracrustal associations of tholeiitic meta-basaltic, meta-sedimentary, and ultramafic rocks, all variously metamorphosed at amphibolite–granulite facies (e.g., Friend and Nutman 2005; Garde 1990, 2007; Windley and Garde 2009). The NAC thus provides the opportunity to investigate Archaean crustal growth, in particular using temporally constrained geochemical tools sensitive to source and crustal differentiation processes, such as the Lu–Hf isotopic system deployed here.

The Nuuk region of southern West Greenland (Fig. 1) includes the most extensive tract of Eoarchaean crust exposed on Earth: the Itsaq Gneiss Complex (Nutman et al. 1996), as well as younger orthogneiss units. The gneisses cropping out within the Nuuk region have been sub-divided into a number of distinct terranes, largely on the basis of geochronology and structural relationships (e.g., Friend and Nutman 2005). The Akia Terrane is one of the most northerly of these crustal blocks, and is largely comprised

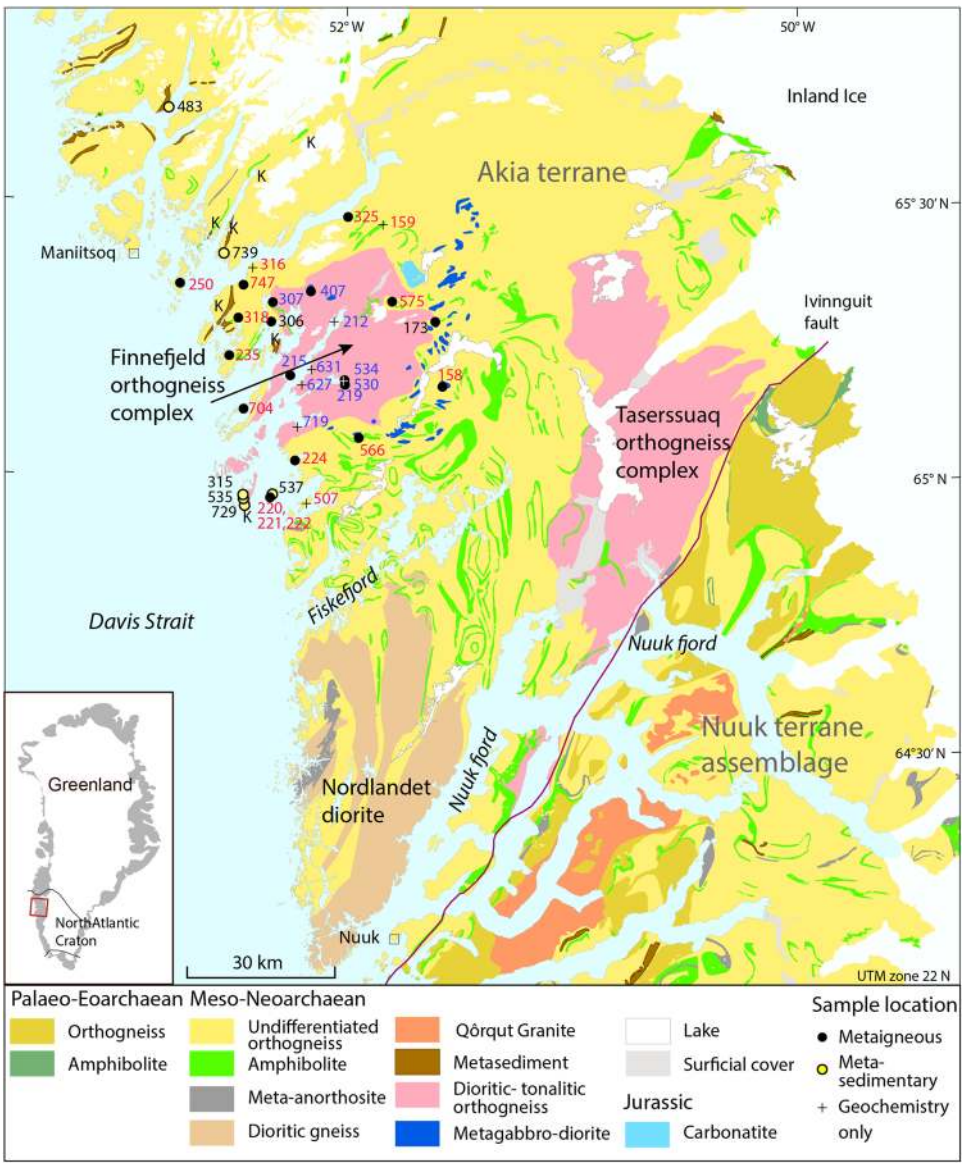

Fig. 1 Geological map of the Nuuk region, with major terranes marked, and samples for this study identified. Samples from the Finnefjeld Orthogneiss Complex are in blue text, and those samples from outside in red text. Crosses represent samples for which only geochemistry is reported. K = outcrops of Kangerluarsuk supracrustal rocks. Geology based on geological maps published by Geological Survey of Greenland with revision of the Nuuk terrane assemblage according to Nutman et al. (2015)

of Mesoarchaean dioritic and tonalitic orthogneisses and supracrustal successions, with later minor magmatism (e.g., Garde 1997; Steenfelt et al. 2005). To date, however, there have been few Hf isotope studies from across the NAC, and these are especially lacking with respect to providing a better understanding of the genesis and evolution of the volumetrically significant Meso-to-Neoarchaean crustal growth and reworking which served to stabilize the craton.

In this contribution, we report zircon U–Pb and Lu–Hf isotope data, and major and trace element whole-rock geochemistry, from a range of meta-igneous intrusive rocks sampled from within the northern part of the Akia Terrane. We also report U–Pb and Lu–Hf isotope data in zircons from metasedimentary rocks sampled from supracrustal successions, cropping out within the same region. We interrogate the data for crustal evolution trends through time with respect to the nature of source and conditions of melting, and use this information to elucidate the generation of this crust and its subsequent modification, with implications for the development of Mesoarchaean terranes.

Regional geology

The Nuuk region in southern West Greenland (Fig. 1) is a component of the NAC, and is a classic example of Archaean horizontal tectonics and terrane accretion (e.g., Bridgwater et al. 1974; Friend et al. 1988; Windley and Garde 2009). The NAC is largely comprised of Palaeo-to-Neoarchaean orthogneisses, compositionally dioritic–TTG, with intercalated supracrustal successions of mafic metavolcanic and rare meta-sedimentary rocks, all variously metamorphosed to amphibolite and granulite facies (Friend and Nutman 2005; Kalsbeek and Garde 1989). Minor components include gabbro-anorthosite, diorite, and ultramafic sequences.

Eoarchaean gneiss complexes occur within West Greenland in three recognized tectono-metamorphic terranes: Færingehavn, Isukasia, and Aasivik (Friend and Nutman 2005). In addition, four Palaeo-to-Mesoarchaean gneiss terranes in the central NAC are also identified: Tre Brødre, Tasisuarsuaq, Kapisilik, and Akia (Friend et al. 1987; Næraa and Scherstén 2008). These terranes are interpreted to have had their final assembly and suturing by granites during the latest Neoarchaean (Friend et al. 1996; Nutman et al. 2007).

The Akia Terrane

The Mesoarchaean Akia Terrane is one of the northern-most crustal blocks identified within the NAC (Fig. 1) (Friend et al. 1988; McGregor et al. 1991), and was built through at least two major phases of crustal growth. A dioritic phase—the Nordlandet diorite—is mainly exposed in the southern Akia Terrane, due south of Fiskefjord (Fig. 1), where it has yielded zircon $^{207}Pb/^{206}Pb$ magmatic ages of 3.22–3.18 Ga (Garde et al. 2000). The magmatic record implies that after a hiatus of ca. 130 Ma, the emplacement of extensive tonalitic crust occurred, a period of rapid and voluminous magmatism, dated through zircon U–Pb geochronology between 3.05 and 3.02 Ga (Garde et al. 2000, 2012b). This tonalitic crust dominates the Akia Terrane north of Fiskefjord.

The tonalitic components now crop out as orthogneiss, and are tectonically intercalated with supracrustal rocks and associated mafic–ultramafic intrusive complexes. A recently proposed unit of supracrustal rocks in the Maniitsoq region, informally known as the Kangerluarsuk supracrustal belt (Fig. 1), consists largely of heterogeneous, compositionally layered meta-basalts, meta-pelite–meta-psammite sequences, with siliciclastic components. The Kangerluarsuk supracrustal belt has detrital zircon ages indicating deposition between 2.88 and 2.86 Ga (Kirkland et al. 2018a), similar in age to the ca. 2.8 Ga Storø Supracrustal Belt cropping out further south (Szilas et al. 2014). Supracrustal rocks are also found intercalated with meta-gabbronoritic and ultramafic rocks that may represent layered intrusive complexes (Szilas et al. 2015). The supracrustal rocks found in the Akia Terrane are interpreted as remnants of arc-related oceanic crust, a model which has the precursor to the orthogneiss intruded within a convergent plate-tectonic setting (Garde 1990, 1997; Garde et al. 2000; Szilas et al. 2017). Phase equilibria modelling of metapelites from the Kangerluarsuk supracrustal belt suggests that after deposition, these rocks were buried to > 30 km depth, where they experienced partial melting at ~ 820–850 °C and 8–10 kbar in the period 2.86–2.70 Ga (Kirkland et al. 2018a).

In accord with the current interpretation of a predominantly horizontal geodynamic regime during the formation of the NAC, it has been proposed that the 3.0 Ga tonalitic gneisses of the Akia Terrane had their petrogenesis through slab melting of subducted oceanic crust (e.g., Garde 1997; Winther and Newton 1991). The model of Garde et al. (2000) has the Akia Terrane developing by inception of a ca. 3.1 Ga magmatic arc over an older Mesoarchaean crustal nuclei. In this model the arc, exposed in Nuuk Fjord (Godthåbsfjord) and the Qussuk peninsula, and dated to ca. 3.075 Ga on the basis of zircon sourced from volcanosedimentary sequences, is inferred to have generated intermediate and subordinate felsic volcanic rocks (Garde 2007; Garde et al. 2012a; Szilas et al. 2017). Then, the arc, and underlying dioritic crust, was intruded by voluminous TTG gneisses in the period 3.06–3.02 Ga (Garde 1990, 1997; Garde et al. 2000). Low-pressure granulite facies metamorphism followed swiftly thereafter at 2.99–2.975 Ga (Friend and Nutman 1994; Garde 2007; Garde et al. 2000), an event which resulted in widespread partial melting evidenced by two-pyroxene leucosomes in dioritic–mafic gneisses. This

metamorphism was synchronous with the emplacement of late-tectonic tonalitic intrusions at 3.01–2.97 Ga, including the Taserssuaq Tonalite, Finnefjeld Gneiss, and the Qugssuk and Igánánguit granites (Garde 1997; Garde et al. 2000; Scherstén and Garde 2013). However, a second model has also been proposed for the development of the northern Akia Terrane, that of a giant bolide impacting at ≥ 3.0 Ga, resulting in prolonged Mesoarchaean thermal reworking, and a range of melting and cataclastic deformation features and inferred hydrothermal alteration across the region (Garde et al. 2012a).

The NAC subsequently experienced terrane assembly and minor Neoarchaean granitic magmatism. To the north, the Akia Terrane is bounded by the (latest) Meso-to-Neoarchaean Tuno terrane (Friend and Nutman 1994; Yi et al. 2014). To the south, it is juxtaposed against several Eo-to-Mesoarchaean terranes of the Nuuk region, which amalgamated in the early Neoarchaean (Friend and Nutman 2005; Friend et al. 1996) ("Nuuk terrane assemblage", Fig. 1). Later events include Palaeo- and Neoproterozoic rifting and dyke emplacement (Berthelsen 1962; Bridgwater et al. 1995; Cadman et al. 2001; Nutman et al. 1999), the intrusion of Neoproterozoic kimberlite dykes, and finally a Jurassic carbonatite complex (Larsen and Rex 1992; Tappe et al. 2011).

The Finnefjeld Orthogneiss Complex

The Finnefjeld Orthogneiss Complex crops out over a broadly circular region ~ 30 km in diameter, within the northern Akia Terrane (Fig. 1). It is comprised of a leucocratic orthogneiss, termed the Finnefjeld Gneiss (Berthelsen 1962; Garde et al. 2014). This unit has minor mafic enclaves, but which are less common than observed within the surrounding tonalitic gneisses. Here we refer to the gneiss unit as the Finnefjeld Orthogneiss Complex (FOC), since it comprises several generations of dioritic–granitic gneiss. This poly-phase intrusive complex has as a dominant component a homogeneous leucocratic, medium–coarse-grained, occasionally porphyritic (porphyroblastic), hornblende and biotite bearing quartz dioritic–granodioritic rock (Berthelsen 1962). Although the FOC has been ductilely deformed, it is less deformed than, and distinct from, the surrounding multiply deformed and mafic enclave-rich complex of tonalitic and dioritic orthogneisses which volumetrically dominate the Akia Terrane.

The FOC has previously been considered to represent either (a) the intrusion of a dome-shaped tonalitic body into the banded ca. 3.0 Ga TTG-suite gneisses which comprise the majority of the Akia Terrane (e.g., Marker and Garde 1988; Steenfelt et al. 2005); or (b) their subsequent reworking during a later thermal event, most recently reinterpreted as a domain of cataclasis and remelting following a bolide impact (Garde et al. 2012a).

Samples

To characterize the crust which makes up the northern Akia Terrane, 27 samples of both meta-igneous (mafic–felsic), and meta-sedimentary rocks, were taken from a range of localities across the Maniitsoq region, including from within, and thus considered representative of, the FOC (Fig. 1). These samples were analyzed for zircon U–Pb and Lu–Hf isotopes, and a subset of igneous samples for whole-rock major and trace element geochemistry. U–Pb geochronology for samples 158, 250 and 747 is reported in Kirkland et al. (2016); Hf isotopes from these previously dated zircons are reported here. An additional eight samples of igneous rocks were analyzed for whole-rock major and trace element geochemistry only. Table 1 summarizes sample lithologies, location, and U–Pb ages and Lu–Hf isotope data, where available.

Meta-igneous samples

Samples 220, 221 and 222 are from the same locality on an island off the west coast (Fig. 1). All three samples were taken from a low strain zone within a fold hinge, hence the rock relationships are well constrained due to the relatively weak deformation. Sample 220 is a dioritic gneiss, which we interpret to represent an outlier of the Nordlandet diorite which crops out extensively further south (Fig. 1). Sample 222 is a trondhjemitic phase with an intrusive relationship into both the diorite (220; outcrop photograph Fig. 2a) and an amphibolite, and thus is interpreted as a younger magmatic phase. Sample 221 is a later granitic dyke that cross-cuts all other lithologies at this locality.

A number of the samples taken are representative of the tonalitic orthogneiss which volumetrically dominates the northern Akia Terrane (sample numbers 566, 575, 158, 325, 235, 250, 306 and 747). Figures 2b, c show typical outcrop patterns for this rock type (samples 235 and 306, respectively). A thin section photomicrograph of tonalite sample 747 is shown in Supplementary Figure S1A. This sample contains a weak–moderate foliation defined by the parallel alignment of biotite and the sample is dominated by subhedral plagioclase (~ 60 vol.%) with subordinate quartz (~ 30 vol.%) and biotite (~ 10 vol.%).

Samples 173, 215, 307, 407, 530 and 534 are all components of the Finnefjeld Orthogneiss Complex (Fig. 1). Samples 407 and 534 are samples of the leucocratic phases of the FOC; 307 and 530 are dioritic phases (Fig. 2d is of

Table 1 Summary of samples, lithologies, locations, zircon U–Pb ages and mean Hf isotopes

Sample ID	Lithology	Latitude	Longitude	Age (Ma, 2σ)	εHf (1σ)
Meta-igneous samples					
220	Diorite	64.97035	− 52.29851	3231 ± 5	− 1.2 ± 1.6
222	Trondhjemite	64.97035	− 52.29851	3240 ± 8	− 4.0 ± 2.0
306	Tonalite	65.29019	− 52.30963	3019 ± 12	− 1.6 ± 0.8
566	Tonalite	65.08117	− 51.92203	3018 ± 13	− 1.5 ± 1.0
575	Granite	65.32964	− 51.78435	3013 ± 16	− 2.4 ± 1.5
158	Tonalite	65.17606	− 51.56314	3008 ± 9‡	− 2.5 ± 0.8
221	Granite	64.97035	− 52.29851	2977 ± 7	− 7.0 ± 1.8
224	Granite	65.03800	− 52.19400	2986 ± 8	− 2.2 ± 1.0
235	Tonalite	65.22751	− 52.48842	2992 ± 7	− 3.9 ± 1.9
250	Tonalite	65.35717	− 52.71120	2998 ± 16‡	− 3.2 ± 1.5
325	Tonalite	65.48295	− 51.98221	3002 ± 13	− 1.7 ± 0.5
747	Tonalite	65.35616	− 52.43367	2990 ± 7‡	− 1.5 ± 0.6
704	Pegmatite	65.13022	− 52.42159	2729 ± 9	− 7.6 ± 1.0
318	Pegmatite	65.29624	− 52.45278	2729 ± 11	− 4.9 ± 1.2
507	Tonalite◊	64.96360	− 52.14213		
159	Tonalite	65.47260	− 51.82899	3019 ± 11	
316	Tonalite◊	65.39074	− 52.39485		
173	Leucogabbro*	65.29379	− 51.59563	3007 ± 9	− 2.4 ± 0.9
307	Diorite–tonalite*	65.32594	− 52.30472	3011 ± 10	− 2.3 ± 2.5
534	Granite*	65.18602	− 51.98658	2999 ± 5	− 2.8 ± 1.2
530	Diorite*	65.17720	− 51.98555	2998 ± 6	− 2.9 ± 2.3
407	Tonalite*	65.34633	− 52.13923	2994 ± 5	− 2.7 ± 2.1
215	Granite*	65.19257	− 52.22268	2558 ± 8	− 12.2 ± 1.0
212	Tonalite*◊	65.29507	− 52.03476		
219	Tonalite*◊	65.18705	− 51.99236		
570	Tonalite*◊	65.13620	− 51.90170		
627	Tonalite*◊	65.17939	− 52.17053		
631	Tonalite*◊	65.20760	− 52.12929		
719	Tonalite*◊	65.10191	− 52.18739		
Metasedimentary samples					
739	Psammite	65.41284	− 52.52253	≥ 2958 ± 10	− 1.9 to − 4.1
729	Psammite	64.95424	− 52.40747	≥ 2891 ± 26†	0.3 to − 6.7
535	Paragneiss	64.96708	− 52.41281	≥ 2924 ± 16	− 0.6 to − 4.7
483	Paragneiss	65.67670	− 52.78071	2729 (m)	− 2.4 to − 4.7
537	Paragneiss	64.97586	− 52.28866	≥ 2970 ± 14	− 0.3 to − 5.0
315	Psammite	64.97409	− 52.41509	≥ 2877 ± 22†	4.2 to − 7.5

Maximum depositional age is quoted for metasedimentary samples, except for sample 483 where a metamorphic age (m) is given

*Sample taken from the Finnefjeld Orthogneiss Complex (FOC)

‡Ages from Kirkland et al. (2016)

†Ages from Kirkland et al. (2018a)

◊Samples for which only whole-rock geochemistry is reported

sample 307 and Fig. 2e shows a leucocratic phase). Sample 407 is dominated by blocky quartz and feldspar with large phenocrysts of hornblende (Fig. S1B). Sample 534 is a biotite tonalite with a foliation defined by the alignment of biotite and elongate recrystallized quartz (Fig. S1C). Sample 173 is a two-pyroxene leucogabbro with plagioclase (~ 50 vol%) and quartz (~ 10 vol%) (Fig. S1D).

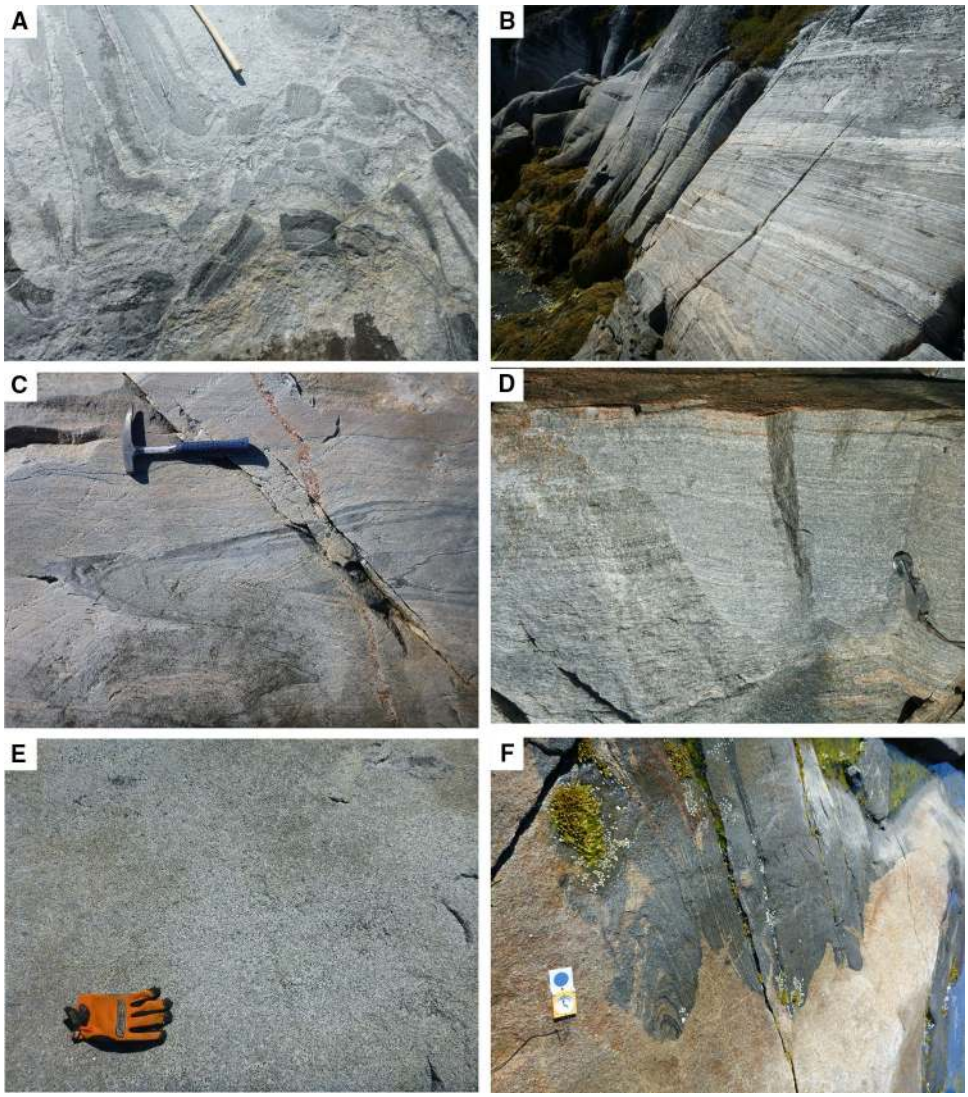

Fig. 2 Field photos. **a** Outcrop photo of samples 220 and 222. Sample 220 is a diorite, and 222 is a tonalitic phase with an intrusive relationship into diorite 220; **b, c** outcrop photos of the tonalitic orthogneiss which dominates the northern Akia Terrane. **b** is of sample 235 and **c** of sample 306; **d, e** Representative outcrop photos of the Finnefjeld Orthogneiss Complex; **d** is of sample 307, and **e** a more leucocratic phase. **f** Late stage 2.5 Ga granite, sample 215

Samples 318 and 704 are pegmatites which cross-cut the tonalitic orthogneiss, and sample 215 is a late-stage cross-cutting granitic phase (Fig. 2f).

Meta-sedimentary samples

Samples of six metasedimentary rocks were taken (Nos 315, 483, 535, 537, 729, 739), ranging in lithology from psammite to paragneiss (including migmatitic components). All of these samples are units of the informally named Kangerluarsuk supracrustal belt (Kirkland et al. 2018a), which is primarily found cropping out along the coastal regions of the northern Akia Terrane (Fig. 1).

Sample 315 is a meta-psammite comprising quartz, feldspar, amphibole and biotite. Leucosomes are well-developed throughout the outcrop, although these were avoided during sampling. This quartzo-feldspathic unit represents the most felsic component of a supracrustal sequence dominated by rusty-weathering amphibolites. The zircons separated from sample 315 have been previously analyzed for U–Pb geochronology, the cores yielding $^{207}Pb/^{206}Pb$ ages of between 3189 and 2877 Ma, and the rims yielding younger ages of 2582 ± 24 and 2550 ± 30 Ma (2σ) interpreted as the timing of later high-grade metamorphic events affecting the unit (Kirkland et al. 2018a).

Sample 729 is a meta-psammite taken from a coastal outcrop of folded felsic paragneiss interlayered with mafic meta-volcanic schist, and is found within the same supracrustal sequence as sample 315. Garnet–bearing leucosomes are present throughout this meta-sedimentary sequence, indicative of in situ partial melting. Kirkland et al. (2018a) also reported U–Pb analyses of zircons from sample 729, which yielded $^{207}Pb/^{206}Pb$ ages between 3199 and 2891 Ma, with a youngest concordant age of 2891 ± 26 Ma (2σ), taken as the maximum depositional age of this unit.

Samples 535 and 537 are both migmatitic paragneisses. In thin section, sample 535 has two domains: (1) a coarser-grained domain dominated by quartz and blocky plagioclase with rare biotite, and (2) a finer grained region with more biotite (~10 vol.%). Sample 537 is medium grained (1–2 mm) and dominated by plagioclase (~50 vol.%), quartz (~30 vol.%) and biotite (~20 vol.%). The parallel alignment of biotite defines a moderate foliation in this sample. Quartz contains irregular grain boundaries and undulose extinction, which indicates significant dynamic recrystallization. Biotite is euhedral and found along grain boundaries.

Sample 739 contains a fine-grained (< 0.5–1 mm) mineral assemblage of plagioclase (~40 vol.%), quartz (~40 vol.%), biotite (~10 vol.%), amphibole (~5 vol.%) and minor K-feldspar (~5 vol.%). K-feldspar (microcline) is found along grain boundaries between quartz and plagioclase and sometimes surrounds corroded biotite (Fig. S1E). The low dihedral angles of some K-feldspar are consistent with it representing a remnant of anatectic melt (Fig. S1F).

Analytical methods

U–Pb geochronology on undated samples was performed using in situ analytical techniques on zircon separates. Zircon grains were separated using magnetic and heavy liquid techniques. The zircons, together with reference standards, were cast in epoxy mounts, which were then polished to approximately a half-grain thickness for analysis. Each

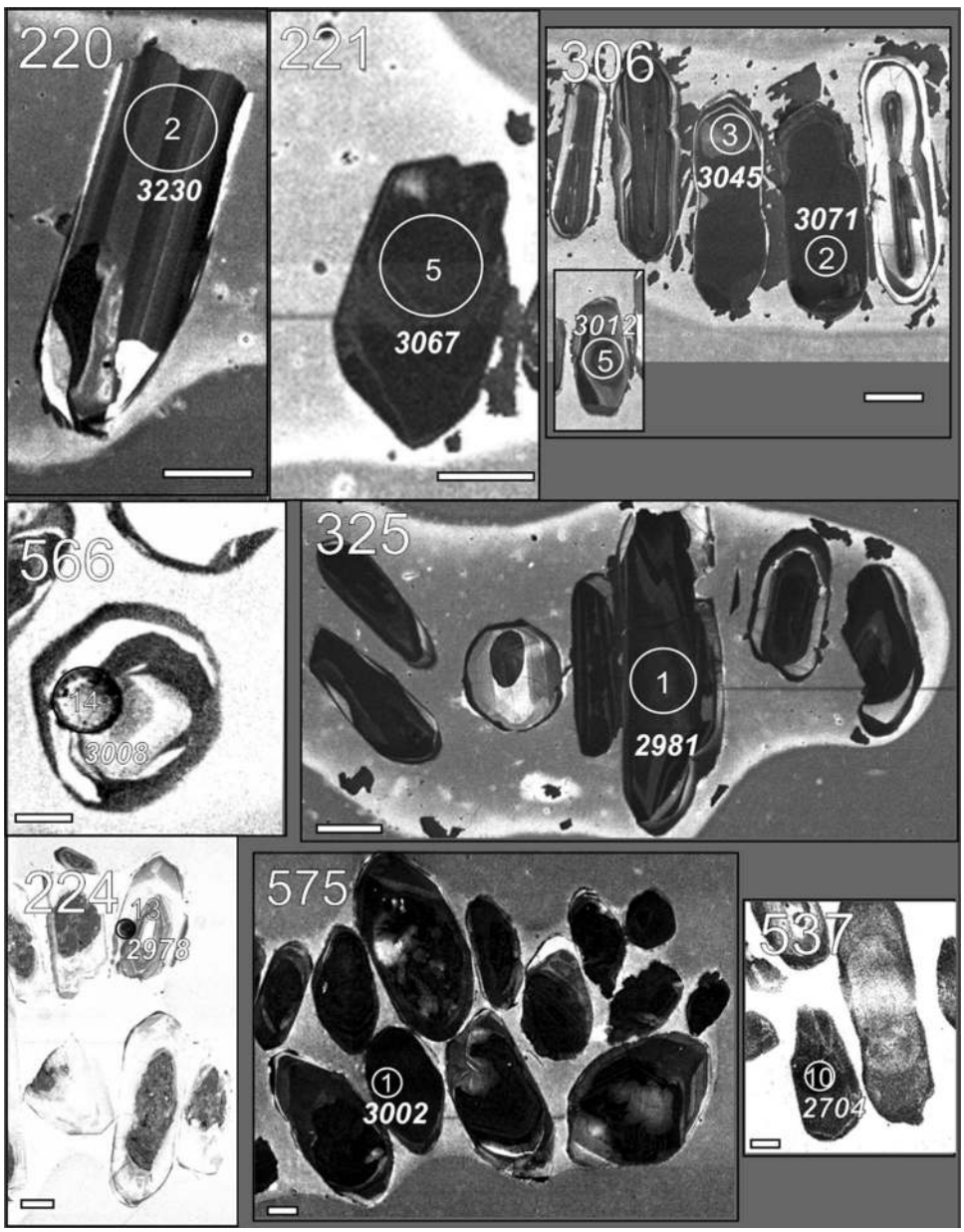

Fig. 3 Representative cathodoluminescence images of zircon grains from selected samples, highlighting U–Pb analyses (age in Ma). Scale bar is 50 µm long

mount was documented with transmitted and reflected light micrographs and cathodoluminescence (CL) images prior to analysis. Figure 3 shows representative CL images of selected zircon grains, and all CL images are in the Supplementary Data. Combined U–Pb geochronology and Lu–Hf isotope analysis of all but one sample was performed at the John de Laeter Centre of Mass Spectrometry, Curtin University, using split-stream combined LA-ICPMS (U–Pb; quadrupole-based analytical sessions) and multi-collector LA-ICPMS (Lu–Hf) techniques. Geochronology of sample 212 was undertaken separately using SIMS (SHRIMP), also at the John de Laeter Centre of Mass Spectrometry, with follow up LA-ICPMS Lu–Hf isotope analyses located on the SIMS spots. Detailed descriptions of the analytical methodologies are provided in the Supplementary Data.

Whole-rock compositions were determined at ALS Laboratories (Ireland) using their ME-ICP06 analytical package for major oxides. Samples were digested by lithium metaborate fusion and major element concentrations were determined by ICP-AES. Trace element concentrations were determined by ICPMS using the ME-MS81 and ME-MS61 packages.

Results

Zircon U–Pb geochronology

Supplementary Table S1 details U-Pb analytical results, from both LA-ICPMS and SIMS sessions. Isotope analyses were categorized as either igneous (group I), metamorphic (M), detrital (S), or xenocrystic (X) on the basis of zircon texture (imaged through CL) and age context. Figure 4a shows a stacked U–Pb concordia plot for all meta-igneous samples, and Fig. 4b for meta-sedimentary samples. A summary of age data is given below; analyses > 10% discordant (on the basis of percent difference between the calculated individual $^{238}U/^{206}Pb$ and $^{207}Pb/^{206}Pb$ ages) were excluded from sample-level age calculations. Detailed geochronology for each sample is in the supplementary data. All uncertainties are reported at 2σ unless otherwise stated.

Meta-igneous samples

Two samples have U–Pb ages similar to that of the ca. 3.2 Ga dioritic component cropping out further south. Sample 220 has a magmatic age of 3230 ± 5 Ma, while zircons taken from sample 222 have an age of 3240 ± 8 Ma, interpreted as reflecting assimilation of the older dioritic gneiss, a conclusion substantiated by it having an intrusive relationship to sample 220. A single rim analysis from sample 220 yielded a younger age of 3025 ± 9 Ma, interpreted as the age of crystallization. Sample 221 is a cross-cutting granitic dyke taken from the same locality as 220 and 222, and a $^{207}Pb/^{206}Pb$ age of 2977 ± 7 Ma was calculated for this sample. The zircon textures for sample 221 indicate significant reabsorption and regrowth and/or recrystallization (Fig. 3), and this age may reflect a metamorphic event.

Samples of the dominant tonalitic orthogneiss yielded magmatic crystallization ages of between 3019 and 2910 Ma. In addition, sample 325 hosted xenocrystic zircon components which have ages of 3157–3092 Ma. Some samples also preserved 2821–2816 Ma metamorphic zircon overgrowths (Fig. 3). The five felsic samples interpreted as

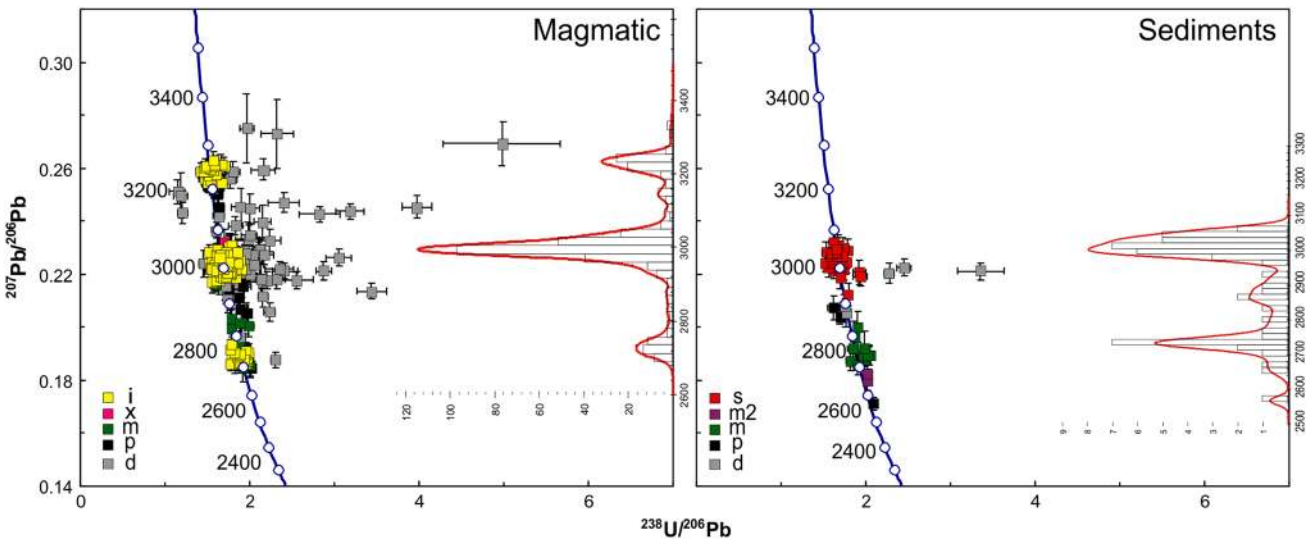

Fig. 4 **a** U–Pb concordia plot for all meta-igneous samples; **B** U–Pb concordia plot for all meta-sedimentary samples. Group identification: *I* igneous; *M* (*M2*) metamorphic; *S* detrital; *X* xenocrystic; *P* concordant, but interpreted to have lost radiogenic Pb; *D* discordant

belonging to the FOC yielded magmatic ages ranging from 3011 to 2993 Ma.

Sample 224, a granite, yielded a weighted mean $^{207}Pb/^{206}Pb$ age of 2986 ± 8 Ma, interpreted as the age of magmatic crystallization. These analyses indicate moderate Th/U ratios (~0.54) and are located on textures indicative of primary magmatic growth (Fig. 3). In addition, leucogabbro sample 173 yielded a magmatic age of 3007 ± 9 Ma, and sample 307, a dioritic tonalite, also recorded a magmatic age of 3011 ± 10 Ma.

Three samples were interpreted as representing later, minor Neoarchaean magmatism. Two pegmatite samples, 318 and 704, yield younger ages of 2729 ± 11 Ma and 2729 ± 9 Ma, respectively, both interpreted as the crystallization age of the rock. The youngest sample, 215 is a late undeformed granite within the FOC, and this yielded a magmatic $^{207}Pb/^{206}Pb$ age of 2558 ± 8 Ma.

We report U–Pb data on four samples interpreted to be meta-sedimentary. Analyses from paragneiss sample 483 yield a $^{207}Pb/^{206}Pb$ age of 2729 ± 11 Ma, interpreted as the age of high-grade metamorphism, and these analyses have generally low Th/U ratios of ~0.78. For sample 535, six analyses of zircon cores yielded $^{207}Pb/^{206}Pb$ ages of 3008–2924 Ma, interpreted as the age of detrital components, while younger ages (2798 ± 30 Ma, 2664 ± 25 Ma, and 2567 ± 12 Ma) were all interpreted as the timing of high-grade metamorphism. For sample 537, concordant $^{207}Pb/^{206}Pb$ ages of 3049–2970 Ma are interpreted as the age of detrital components. A single texturally homogeneous zircon analysis yielded a $^{207}Pb/^{206}Pb$ age of 2704 ± 16 Ma, interpreted as dating a high-grade metamorphic event (Fig. 3). Psammite sample 739 has detrital components with ages of 3065–2973 Ma, with the maximum age of deposition of the sedimentary protolith as 2958 ± 10 Ma.

Zircon Lu–Hf isotopes

Full zircon Hf isotope analytical results are presented in Supplementary Table S2. The decay constant of Scherer et al. (2001) was used in the calculation of initial Hf isotope ratios. Hf isotope analyses paired with concordant U–Pb are shown on an evolution plot in Fig. 5 for all magmatic samples.

Analyses from zircons from igneous rocks with U–Pb ages of ca. 3.2 and 3.0 Ga have mostly chondritic–subchondritic Hf isotope values (Fig. 5), ranging from approximately + 2 to − 10 epsilon units. The younger magmatic phases (ca. 2.7 and 2.5 Ga), have consistently more evolved Hf isotope values, as low as -14 epsilon units for the youngest phase.

Whole-rock geochemistry

Supplementary Table S3 details whole-rock major and trace element geochemistry for those igneous samples analyzed. To provide a more complete comparison between the 3.0 Ga tonalitic orthogneiss "country rock" (henceforth "tonalite"), and the 3.0 Ga TTG samples of the FOC, we include geochemical analysis from eight additional samples, all of which are components of the same 3.0 Ga magmatic event, and identified in Table 1.

Selected major and trace element plots for the same set of orthogneiss samples are shown in Fig. 6. All the samples fall within the TTG/adakite field of Martin (1986), but a plot of Sr/Y versus Y shows a significant difference in the trends of the two groups of orthogneiss, although there is some overlap between the groups. In terms of major element variations, the two groups of orthogneiss are distinct in that the FOC samples are less evolved with respect to most major

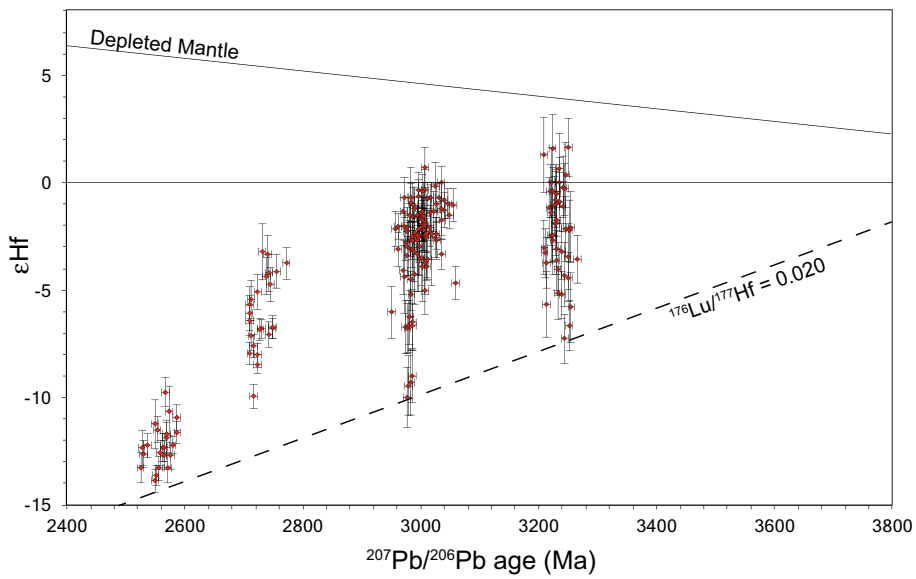

Fig. 5 Hf isotope evolution plot showing calculated εHf versus $^{207}Pb/^{206}Pb$ magmatic age on a per analysis basis, for all magmatic samples. Evolution line defined by $^{176}Lu/^{177}Hf$ of 0.020 is for average mafic crust, perhaps the source to the 3.2 and 3.0 crust

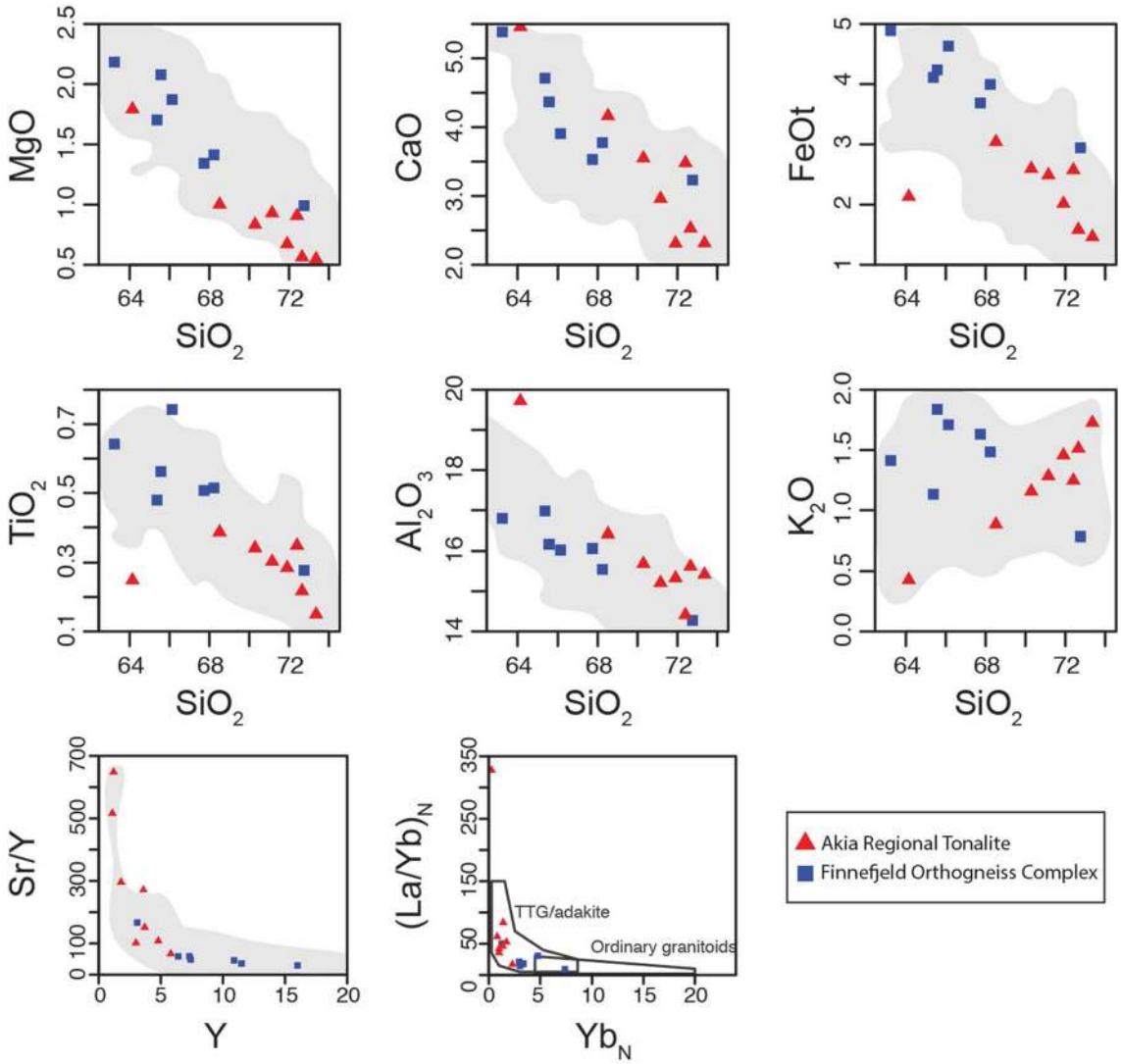

Fig. 6 Whole-rock trace and major element plots for samples of the tonalitic orthogneiss "country rock" (red triangle) and TTG-like samples of the Finnefjeld Orthogneiss Complex (blue square). The grey shading is the range of TTG analyses from the database of Moyen and Martin (2012)

elements by having systematically lower SiO_2 and higher MgO and CaO than the more evolved tonalite; titanium is lower in the tonalite.

Figure 7 shows chondrite-normalized REE, and primitive mantle (PM)-normalized trace element diagrams for the two sets of orthogneiss samples. The most obvious feature is the positive Eu-anomaly recorded in the tonalite, which is not as pronounced in the FOC. The other key difference between the two groups of orthogneiss is the generally lower abundances of HREE in the tonalite, whereas the FOC orthogneiss have abundances of up to ten times that of chondrite for the HREEs. The PM-normalized trace element diagram in Fig. 7 displays several pronounced positive anomalies (Ba–U–La–Pb–Sr–Zr) for both groups of orthogneiss. Thorium shows remarkable variation extending from 1 to about 100 times the chondrite abundance.

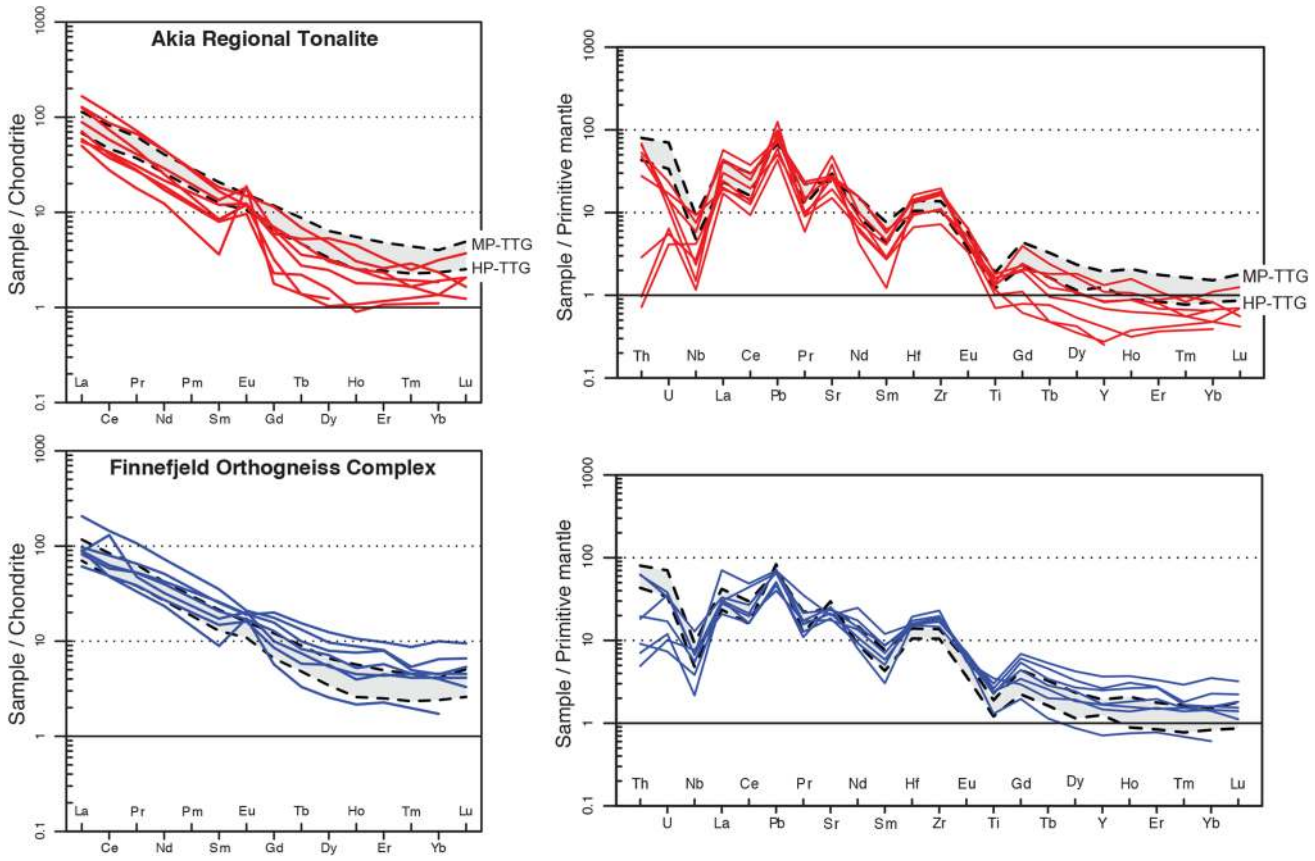

Fig. 7 Trace element plots for samples of the tonalitic orthogneiss (red) and TTG-like samples of the Finnefjeld Orthogneiss Complex (blue). The chondrite-normalized rare earth element (REE) plot uses the values of Anders and Grevesse (1989). The Primitive Mantle-normalized trace element spider diagram uses the values of Palme and O'Neill (2003). Table S3 details the whole-rock geochemistry for those samples plotted here. Representative medium-*P* (MP-TTG) and high-*P* (HP-TTG) TTG compositions of Moyen and Martin (2012) are also plotted for comparison

Discussion

Phases of crustal growth and reworking

Zircon U–Pb geochronology highlights that four magmatic episodes are recorded in the igneous rocks sampled for this study: ca. 3.2, 3.0, 2.7 and 2.5 Ga (Figs. 4, 5). Sample 220, and perhaps sample 222, yield magmatic $^{207}Pb/^{206}Pb$ ages of 3.23 and 3.24 Ga, respectively. We interpret these samples as representative of the Nordlandet diorite, the oldest extant crustal unit found in the Akia Terrane with reported ages of 3.22–3.18 Ga (Garde et al. 2000; Naeraa et al. 2012), and which mainly crops out in the south (Fig. 1). Hf isotope data from samples 220 and 222 record mostly sub-chondritic values, with εHf between + 1.7 and − 7.7, and a mean of − 3.2.

After this early crustal growth phase, zircon U–Pb ages record a hiatus in magmatic activity of ca. 130 Ma, which is then followed by a major, voluminous, intrusive event comprising dominantly tonalitic crust at 3.02–2.98 Ga (Figs. 4, 5). This Mesoarchaean emplacement of what amounts to a significant volume of evolved crust rapidly occurred over a relatively short time period of about 40 Ma (Fig. 4A). The 3.0 Ga tonalitic orthogneiss from the Maniitsoq region records sub-chondritic εHf of between + 0.7 and − 9.3, with a mean of − 2.7 epsilon units (Fig. 5), within analytical error of the earlier diorites. Recently reported zircon Hf data (εHf − 3.8 to − 15.1) for the similarly aged ca. 2.97 Ga felsic orthogneisses from the Kapisilik Terrane (Nutman et al. 2015) are significantly more evolved than we find for the Akia Terrane, perhaps implying this crust incorporated a greater proportion of older pre-existing crust of possibly Eoarchaean age, than the Akia tonalites.

The Finnefjeld Orthogneiss Complex

The petrogenetic origin of the FOC can be compared through geochemistry to that of the tonalitic orthogneiss which dominates the northern Akia Terrane. Figure 8a shows a Hf evolution plot separately identifying samples from within the

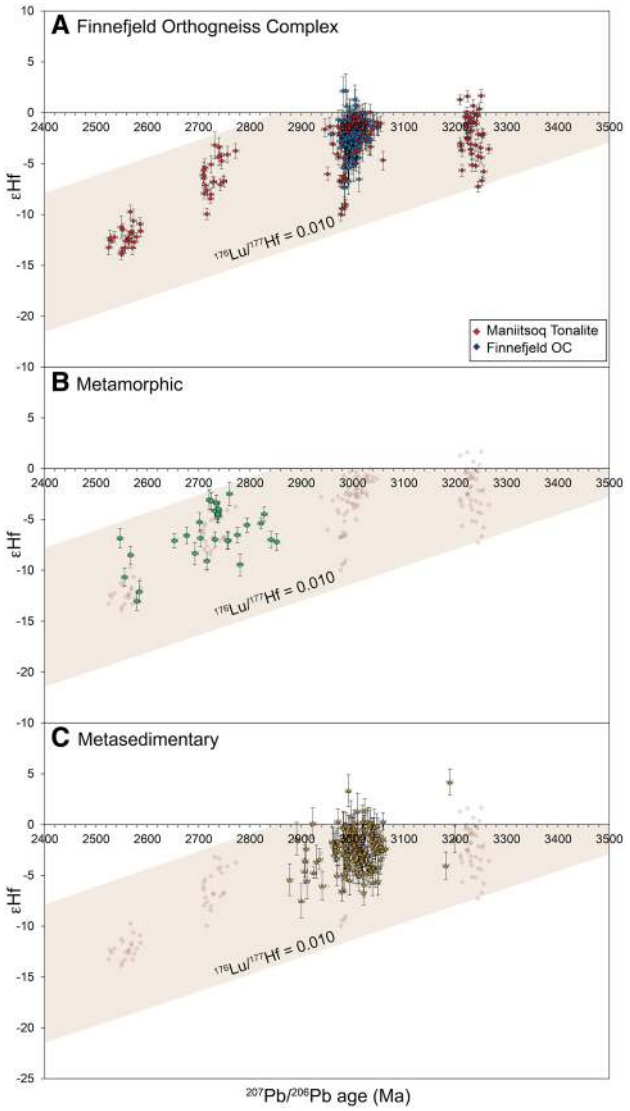

Fig. 8 Individual Hf evolution plots as per Fig. 5 showing **a** Magmatic samples from the Finnefjeld Orthogneiss Complex samples (blue) versus the Akia tonalites (red); **b** Metamorphic samples; **c** Metasedimentary samples. Evolution line with $^{176}Lu/^{177}Hf$ is for average tonalitic crust (e.g., Gardiner et al. 2018)

FOC, and those which characterize the dominant, banded tonalitic "country rock". There is no resolvable age nor Hf isotopic difference between these two sets of samples, with the implication that both units were derived from an isotopically similar magmatic source at a similar time.

Trace element trends for both sets of samples are shown in the PM-normalized plot in Fig. 7, and these highlight some differences in their respective petrogenesis. The obvious positive anomalies for Sr and Eu imply a significant role for plagioclase in the genesis of both the FOC and tonalite, either reflecting plagioclase accumulation during fractionation, or the lack of plagioclase in the source region. However, the marked difference in Sr/Y between the two groups of samples (Fig. 6), in combination with differences in HREE abundances (Fig. 7), is consistent with an interpretation that the FOC formed from melting at lower pressures, where garnet was not stable, than the tonalite, which likely had garnet in the source region.

Comparing these trends with the average medium and high-*P* TTGs of Moyen and Martin (2012) (Fig. 7), the FOC samples have a similar pattern to the medium-*P* baric types, which implies melting in the absence of rutile. In contrast, the tonalite has a higher pressure affinity, with perhaps a greater role for rutile in the source—a feature also hinted at in the more pronounced Ti anomalies, the lower TiO_2 contents, and the generally lower concentrations of Nb (Fig. 6). The interpretation of a shallower melting origin for the FOC samples is also consistent with higher Y concentrations than that measured for the tonalite, as well as lower La/Yb ratios. In a similar fashion, whole-rock major element trends can be interpreted in terms of a combination of both depth, and degree, of partial melting of the source region. The higher MgO and CaO contents in combination with lower SiO_2 (Fig. 6) implies that the FOC perhaps formed through higher degrees of partial melting than the tonalite. The lower SiO_2 content of the FOC implies that it cannot be directly derived from the tonalite, which has a higher SiO_2 content.

In summary, the Hf isotope data and trace element geochemistry for the 3.0 Ga tonalite and the FOC TTG samples, imply a similar source but a different depth, and perhaps degree, of melting. While the tonalite clearly formed from melting within the garnet stability field at some depth (possibly > 10 kbar; Moyen and Stevens 2006), the FOC appears to have resulted from melting within a shallower garnet-free source region (possibly < 10 kbar) (Fig. 7).

The impact model of Garde et al. (2012a) interprets the FOC as having its origin through crustal melting of the surrounding tonalitic orthogneiss along with amphibolite, associated with a massive bolide impact. Melting of the tonalite alone to produce the FOC felsic rocks is not supported with the higher MgO and lower SiO_2 as mentioned above. Furthermore, the overlap of U–Pb ages for the two sets of samples (Fig. 8a) would require this bolide event to have occurred almost simultaneously alongside the production of the tonalitic crust itself proposed to have remelted during impact.

The Taserssuaq Orthogneiss Complex is a large magmatic body within the east of the Akia Terrane, at the northern end of Nuuk Fjord (Fig. 1). It is much larger than the FOC, but is similarly comprised of weakly deformed tonalitic and granodioritic phases, and dated to 2982 Ma (Garde et al. 1986). In the older literature this complex has been mapped as a similar unit to the FOC (e.g., McGregor et al. 1991) and, given the overlap in magmatic ages, and similar rock types, they are probably related. Thus, any model for the formation

of the FOC would likely also have to explain the origin of the Taserssuaq Orthogneiss Complex.

We consider the scenario of a bolide impact as the origin of the FOC to be unrealistic, especially given the likely requirement for it to also explain the origin of the Taserssuaq Orthogneiss Complex. We thus prefer a simpler alternative of the FOC representing coeval intrusion of evolved crust from the same source as the tonalite, but from a shallower melting process. This shallower melting may be structurally controlled, or it may reflect a setting of coeval melting over a substantial lithospheric depth. This simpler model is more aligned with the conclusions of Berthelsen (1962), whose structural work demonstrated that the FOC was perhaps an 'ordinary' part of the local geology.

Nordlandet diorite

The petrogenetic relationship between the 3.2 Ga Nordlandet diorite and the 3.0 Ga tonalite is poorly constrained. The diorite predominates south of Fiskefjord, whilst the tonalite mainly crops out to the north (Fig. 1). The field relationships between diorite sample 220, and trondhjemite (sample 222) (Fig. 2a) highlight an intrusive relationship, and the xenocrystic zircon crystals imply some degree of assimilation of the diorite into the tonalite, at least on a local level. The model of Garde (2007) has tonalite intruding into pre-existing dioritic crust. As noted by Garde (1997), the volumetric extent of the Nordlandet dioritic gneiss found cropping out within the southern part of the Akia Terrane is unusual, both within the NAC and amongst Archaean cratons, and Garde (1997) interpreted its genesis as requiring a mantle component.

Reported whole-rock Sm–Nd isotope data for the Nordlandet diorite plots at a highly radiogenic εNd_{3221} of +4.9 (Garde et al. 2000), above depleted mantle. On the basis of whole-rock major and trace element geochemistry, and age, we interpret sample 220 to be representative of the Nordlandet diorite. If this thesis is correct, it implies a mismatch between the subchondritic Hf and superchondritic Nd isotope analyses recorded for this unit. This disparity may be explained as either: (a) the whole-rock Sm–Nd analysis experienced isotopic disturbance; or (b) a decoupling of the Hf and Nd isotopic systems. Such decoupled Hf–Nd compositions have been measured in Eoarchaean tholeiitic basalts of the Isua supracrustal sequences (Hoffmann et al. 2011b), which have superchondritic Sm/Nd, but slightly subchondritic Lu/Hf. Although the origin of this decoupling is unclear, it may reflect crustal extraction from a highly depleted mantle reservoir (Gardiner et al. 2019).

Later magmatic and metamorphic events

The current geological model for the Akia Terrane (Friend and Nutman 1994; Garde et al. 2000) proposes a rapid high-*T*, low-*P*, granulite-facies metamorphic event to have affected the nascent tonalitic crust immediately on or after its emplacement (ca. 2.97 Ga), although there is only limited geochronological data to constrain the timing and duration of this event. The northern Akia region was then subsequently affected by two widespread, but volumetrically minor, late Archaean thermal events: (a) at 2.86–2.70 Ga, responsible for widespread metamorphism, deformation, and partial melting leading to volumetrically minor melts and the formation of pegmatites (Friend et al. 1996; Kirkland et al. 2018a); and (b) ca. 2.5 Ga expressed by volumetrically minor cross-cutting granitic (*s.s.*) magmatism.

Our isotope data record both these later phases of crustal reworking (Fig. 5). Samples 318 and 704 are examples of the pegmatites, with identical weighted average zircon $^{207}Pb/^{206}Pb$ magmatic ages of 2.73 Ga. Sample 318 records zircon εHf between −3.2 and −7.1; that for sample 704 is slightly more evolved, with εHf between −6.7 and −10.0 (Fig. 5). These data all plot within a Hf evolution trend extrapolated from the 3.0 Ga magmatism ($^{176}Lu/^{177}Hf$ = 0.010), implying the Hf isotopic composition of these pegmatites can largely be attained through reworking of the older 3.0 Ga tonalitic crust. Similar 2.72–2.71 Ga ages of magmatism and metamorphism have been recorded from across the Nuuk region and have been interpreted as resulting from terrane accretion (Friend et al. 1996).

The youngest phase of magmatism recorded in our Maniitsoq samples is a granite (sample 215), for which we date the timing of magmatism to 2.56 Ga. This sample yielded the most evolved Hf isotope data of all the samples, with εHf between −9.7 and −13.9, and a mean of −12.2 (Fig. 5). This sample also plots within the same Hf evolution trend as samples 318 and 704, again implying the granite predominately resulted from reworking of the existing tonalitic crust. The zircon crystallization in sample 215 was coeval with the growth of metamorphic apatite in leucosomes within the TTGs (Kirkland et al. 2018b). Hf isotope data from the similarly aged 2.55 Ga Qôrqut granite, within the Nuuk region, has a slightly more evolved Hf isotopic signature (Hiess et al. 2011; Næraa et al. 2014), interpreted as reflecting melting of an older crustal source than that found outcropping within the Akia Terrane.

Zircon domains from our samples that we interpret as metamorphic growth events have U–Pb ages of between 2.85 and 2.75 Ga. This growth may be attributed to the high-pressure granulite facies event which affected the Maniitsoq region between 2.86 and 2.70 Ga. Kirkland et al. (2018a) interpreted peak *P–T* metamorphic conditions of 820–850 °C and 8–10 kbar, which is sufficient to precipitate

new rims in pre-existing zircon grains. The Hf isotope trends of these metamorphic rims lie within the evolution trend of the 3.0 Ga tonalitic rocks (Fig. 8b), which implies that the Hf incorporated into metamorphic zircon was likely sourced from the dissolution of pre-existing zircon during anatexis, with no breakdown of radiogenic phases, or little time between growth and breakdown (e.g., Flowerdew et al. 2006; Li et al. 2018). We link these metamorphic events to the thermal events associated with magmatic accretion as recorded in the coeval minor magmatism.

Kangerluarsuk supracrustal belt

Zircon grains from the metasedimentary rocks analyzed here are largely considered to be of detrital origin, although some grains may have domains or be discrete crystals representing growth from in situ melt. Recent detrital U–Pb geochronology suggests these metasedimentary successions had their provenance from the surrounding TTGs (Kirkland et al. 2018a). In particular, age peaks at 3.2 and 3.0 Ga were identified, which correlate with the magmatic ages of the Akia diorites and tonalites.

Figure 8c shows a Hf evolution plot for the metasedimentary samples. These data are for the most part identical, in terms of both ages and Hf isotope values, to the 3.0 Ga magmatism. This isotopic similarity supports the interpretation that the clastic units of the Kangerluarsuk Supracrustal Belt were largely sourced from the local TTG successions. Our data also show evidence of detrital zircon grains with younger U–Pb ages, in particular, ages clustering at 2.94–2.88 Ga.

Origin of the Mesoarchaean crust

The continental crust which volumetrically dominates the Akia Terrane is notable for being rapidly generated during two major phases: the diorite at ca. 3.2 and the tonalite at 3.0 Ga (this study, and Garde 1997; Garde et al. 2000; Naeraa et al. 2012). Importantly, no magmatic rocks have been identified from the intervening period. Although an island arc complex, invoked as the setting for the genesis of the 3.0 Ga tonalites, was proposed to be as old as ca. 3.1 Ga in age, this interpretation is largely based on rare zircon U–Pb ages both from a schist, and from xenocrystic zircon cores sourced from meta-volcanic rocks, all found within supracrustal sequences (Garde 2007). The extensive 3.0 Ga tonalitic orthogneiss, including the Finnefjeld Orthogneiss Complex, was all rapidly emplaced within a ca. 40 Ma period of activity (3.05–2.99 Ga).

Tonalitic, and perhaps dioritic, crust is formed from the partial melting of hydrated basalts, i.e. amphibolites, at depth (e.g., Drummond and Defant 1990; Johnson et al. 2014; Rapp 1991). Archaean basalts have Lu/Hf compositions ranging from enriched towards more depleted, chondritic values (Gardiner et al. 2018; Kemp et al. 2010; Smithies et al. 2009). To assess crustal residence times we model the Hf evolution of a (hydrated) basaltic source to the Akia felsic crust, taking a range in $^{176}Lu/^{177}Hf$ for the parent basalt of 0.017–0.024 (Gardiner et al. 2018; Hoffmann et al. 2011b), representing a range in mafic protolith compositions. Projecting these evolution trends back from the minimum and maximum εHf analyses, for both the diorite and tonalite, to a modelled depleted mantle, yields some estimate of crustal residence time—the time since extraction of the parent basalt from the mantle (Fig. 9). The Lu/Hf composition of Eoarchaean mantle

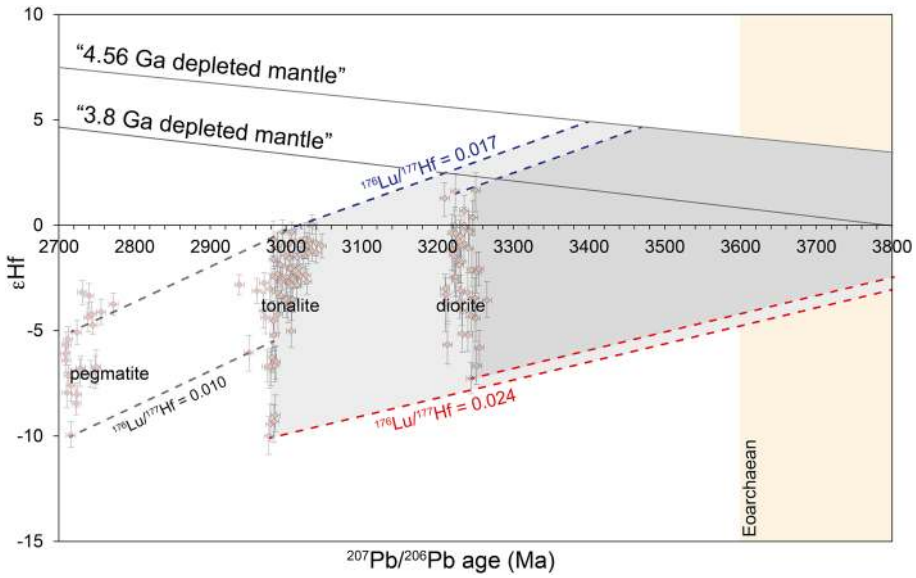

Fig. 9 Hf evolution plot with Lu/Hf evolution trends from both the ca. 3.2 and 3.0 Ga crust forming events, projected back to two different depleted mantle lines. See text for discussion

reservoirs, especially within the context of West Greenland, has been under debate specifically regarding the timing of the onset of mantle depletion. Therefore, both the "4.56 Ga" and "3.8 Ga" modelled depleted mantle evolution trends of Griffin et al. (2000), and Fisher and Vervoort (2018), respectively are plotted on Fig. 9; the latter trend assumes that a chondritic Lu/Hf mantle reservoir persisted until 3.8 Ga.

The most evolved Hf data from both magmatic events clearly implies some incorporation of material which was extracted from the mantle in the Eoarchaean (Fig. 5; Supplementary Figure S3), even taking into account the uncertainties surrounding the application of model ages. Although it is possible that the Eoarchaean component included TTG gneisses, we interpret it to most likely be mafic crust on the basis of a lack of inherited zircon grains yielding appropriate U–Pb ages. Further, the heterogeneous nature of the Hf isotope data implies a mixed source to both the tonalite and diorite: that of a reworking of older Eoarchaean mafic crust with the incorporation of younger, more juvenile, mafic crust, this latter perhaps now represented by the intercalated greenstones found within the Akia orthogneiss. Such Hf isotope heterogeneity is unlikely to result from variable degrees of melting of the mafic sources (Gardiner et al. 2018), probably implying it resulted from different degrees of mixing. The heterogeneity may alternatively originate from a heterogeneous source, but that is difficult to constrain. Notably, there is a geographic trend across the sampling region, with more evolved Hf values predominating in the west (Supplementary Figure S4), implying a regional control to the degrees of mixing of older Eoarchaean crust with juvenile input.

Our Hf data contradicts the previous whole-rock Sm–Nd isotope data on selected tonalite samples from the Akia Terrane (Garde et al. 2000), which records chondritic εNd between 0.0 and − 0.4 (when calculating initial $^{143}Nd/^{144}Nd$ ratios using zircon U–Pb crystallization ages). Garde et al. (2000) used Sm–Nd isochrons to interpret a crustal extraction age for the Akia tonalites of ca. 3.05 Ga. However, this age does not reflect any incorporation of older crust, which may be because a whole-rock approach does not provide the level of precision yielded through individual zircon Hf isotope analyses, or it may reflect heterogeneities between different samples.

In summary, our Hf isotope data strongly argues for the incorporation of some degree of Eoarchaean crust, most likely of mafic composition, in the genesis of the Mesoarchaean Akia crust.

Implications for geodynamic models

Although TTGs are formed from the partial melting of amphibolites at sufficient depths to stabilize garnet and/or amphibole (e.g., Foley et al. 2002; Hoffmann et al. 2011a; Johnson et al. 2014; Rapp 1991), much ongoing debate surrounds the geodynamic settings in which melting occurred to produce such felsic crust. The calc-alkaline affinities of the diorites and tonalites cropping out within the Nuuk region has led workers to propose a subduction origin for their genesis (Garde 1997, 2007; Garde et al. 2000; Steenfelt et al. 2005). However, these so-called "arc-like" geochemical signatures (i.e. Ta and Nb anomalies, and high Sr/Y ratios), which are commonly found in TTG rocks globally, may alternatively originate through infracrustal melting of an enriched basaltic source, within the high geothermal gradients invoked for a vertical tectonic setting during the Eo-to-Palaeoarchaean (Bédard 2006; Johnson et al. 2017).

The East Pilbara Terrane of Western Australia has been critically interpreted as such an example of Archaean vertical tectonics (Hickman 1984; Van Kranendonk et al. 2007), with crustal residence times for Palaeoarchaean TTGs of some 200–700 Ma (Gardiner et al. 2017). Such crustal residence times are greater than that found for oceanic crust on modern Earth, where its longevity is of the order of 200 Ma prior to its destruction at subduction zones (Hawkesworth et al. 2010), and perhaps are significantly more than might be expected during any putative Archaean plate tectonic regime when the mantle was on average hotter (e.g., Herzberg et al. 2010) and mantle convection would have been more vigorous. Long crustal residence times may therefore be interpreted as reflecting the slow development of a volcanic plateau through plume-driven activity, which then infracrustally melts to produce evolved crust (Sizova et al. 2015; Smithies et al. 2009).

The volcanic plateau model thus provides a mechanism for the incorporation of long-lived, older mafic crust in the genesis of younger TTGs. Further, it provides a means for juvenile mafic material to be buried down to the depths where melting occurs through "sagduction" (e.g., Johnson et al. 2014), allowing the mixing of older and younger components. The TTG record from the East Pilbara Terrane also records an episodicity in magmatism (e.g., Gardiner et al. 2017) similar to that recorded within the Akia Terrane. However, whether all this translates to a similar geodynamic model for Mesoarchaean west Greenland is currently debatable. There are no reported enriched basalts of the type invoked as the origin of the Pilbara TTGs. More problematic is explaining the occurrence of a succession of volcaniclastics and amphibolites with an andesitic affinity, as reported south of Fiskefjord (Garde 1997, 2007), although proper determination of their relationship to the dioritic

orthogneiss is hindered by the degree of deformation and metamorphism.

The diorite and tonalite clearly represent separate thermal events. Large-scale Archaean dioritic crust is unusual, and it is curious why the earlier extensive crust-forming event in Akia is dominated by diorite, with the subsequent one by tonalite; they may respectively reflect different degrees of melting of a similar amphibolite source, or perhaps a secular change in geodynamics. Interestingly, our data imply that for the tonalite there is no magmatic age trend across the northern Akia region; these significant volumes of felsic crust were effectively formed in one major geological event.

The development of Mesoarchaean terranes

A key conclusion from this study is that the Mesoarchaean continental crust that forms the Akia Terrane is in part built upon older Eoarchaean crust. A similar inference has been made elsewhere in West Greenland, for the ca. 2.8 Ga Ikkattoq TTG gneisses south of Nuuk which, on the basis of their unradiogenic Nd and Pb isotope compositions, were also interpreted to contain a component of Eoarchaean crust (Friend et al. 2009). This mix of juvenile and older material in the genesis of Mesoarchaean crust contrasts with the dominance of juvenile material inferred for older TTG suites from the Nuuk region, including the Eoarchaean Itsaq Gneisses (Bennett et al. 1993; Hoffmann et al. 2014; Moorbath et al. 1972), although Pb isotope evidence may suggest a component of even older, Hadean material in this ancient crust (Kamber et al. 2003).

A number of studies have used isotopic methods to arrive at the interpretation that, globally, younger Archaean terranes are built on older, long-lived Eoarchaean, or even Hadean, crust (e.g., Kamber 2015). In particular, isotopic studies strongly indicate the involvement of older crustal components in the development of Palaeoarchaean TTGs in both the East Pilbara Terrane (Bickle et al. 1993; Champion and Smithies 2007; Gardiner et al. 2017), and in the Ancient Gneiss Complex and Barberton areas of the Kaapvaal craton (e.g., Amelin et al. 2000; Hoffmann et al. 2016; Kroner et al. 2014; Zeh et al. 2009, 2011).

Building Mesoarchaean terranes on Eoarchaean crustal roots is conceptually straightforward within a volcanic plateau-type setting. Repeated cycles of basaltic volcanism, which buries existing crust to successively deeper crustal levels where it may partially melt and/or drip into the mantle (i.e. "vertical tectonics"), best explains the Hf and Nd isotopic evolution of Palaeo-to-Mesoarchaean crust in the East Pilbara Terrane (e.g., Gardiner et al. 2017). However, the involvement of ancient crust is less easily reconciled with a subduction setting (Johnson et al. 2017). For example, the Mesoarchaean granitic rocks of the West Pilbara Superterrane, which is inferred to have amalgamated with the East Pilbara Terrane during assembly of the Pilbara Craton in a subduction-accretion setting, are geochemically and isotopically juvenile, with no suggestion of any significant Eoarchaean component (e.g., Smithies et al. 2007). Thus, how the presence of a significant component of older Eoarchaean crust in the extensive tonalitic crust of the Akia Terrane can be reconciled with existing models that invoke crustal formation by subduction-accretion is unclear. In summary, we suggest that the involvement of an Eoarchaean root puts important constraints on geodynamic models of the formation of the discrete Palaeo-to-Mesoarchaean terranes that ultimately assembled to form Earth's cratons.

Conclusions

- Two major phases of crust formation at ca. 3.2 Ga (diorite) and 3.0 Ga (tonalite) are recorded in the northern Akia Terrane. Two subsequent minor magmatic events are at ca. 2.7 Ga (pegmatites) followed by late-stage granites at ca. 2.5 Ga.
- Zircon Hf isotopes imply a component of older, Eoarchaean crust in the genesis of both diorite and tonalite, most likely of mafic composition. The Hf isotopes suggest that the 2.7 and 2.5 Ga magmatism both represent reworking of the older tonalitic crust.
- The similarities in U–Pb age and Hf isotope composition between the 3.0 Ga tonalitic orthogneiss and rocks from the Finnefjeld Orthogneiss Complex, imply they were formed from a similar source at a similar time. The magmatic precursor to the Finnefjeld Orthogneiss Complex likely formed by partial melting at shallower conditions outside the stability field of garnet (probably < 10 kbar) than the tonalitic orthogneiss, which probably formed in the presence of garnet. The lower SiO_2 content of the felsic rocks of the Finnefjeld Orthogneiss Complex implies they cannot be directly derived from the surrounding tonalite, which is more evolved.
- These results appear incompatible with the recently proposed impact origin of the Finnefjeld Orthogneiss Complex, and we prefer an alternative explanation of coeval melting of the same magmatic source over a substantial lithospheric depth.
- The involvement of Eoarchaean crust in the growth of the Mesoarchaean Akia Terrane places an important restriction on the development of models for growth and assembly of the North Atlantic Craton.

Acknowledgements The Maniitsoq project is supported by the Ministry of Mineral Resources and Labour, Government of Greenland. NJG thanks Curtin University and Australian Research Council grant FL160100168 for financial support. We thank Clark Friend

for discussions. We also thank Elis Hoffmann and an anonymous reviewer for their helpful comments, and Othmar Müntener for editorial handling.

References

Amelin Y, Lee DC, Halliday AN (2000) Early-middle Archaean crustal evolution deduced from Lu–Hf and U–Pb isotopic studies of single zircon grains. Geochim Cosmochim Acta 64(24):4205–4225

Anders E, Grevesse N (1989) Abundances of the elements—meteoritic and solar. Geochim Cosmochim Acta 53:197–214. https://doi.org/10.1016/0016-7037(89)90286-X

Bédard JH (2006) A catalytic delamination-driven model for coupled genesis of Archaean crust and sub-continental lithospheric mantle. Geochim Cosmochim Acta 70(5):1188–1214. https://doi.org/10.1016/j.gca.2005.11.008

Belousova EA, Kostitsyn YA, Griffin WL, Begg GC, O'Reilly SY, Pearson NJ (2010) The growth of the continental crust: constraints from zircon Hf-isotope data. Lithos 119(3–4):457–466. https://doi.org/10.1016/j.lithos.2010.07.024

Bennett VC, Nutman AP, McCulloch MT (1993) Nd isotopic evidence for transient, highly depleted mantle reservoirs in the early history of the Earth. Earth Planet Sci Lett 119:299–317

Berthelsen A (1962) Structural studies on the pre-Cambrian of western Greenland III. Southern Sukkertoppen district. Bull Gronlands Geol Undersogelse 31:47

Bickle MJ, Bettenay LF, Chapman HJ, Groves DI, McNaughton NJ, Campbell IH, de Laeter JR (1993) Origin of the 3500–3300 Ma calc-alkaline rocks in the Pilbara Archaean: isotopic and geochemical constraints from the Shaw Batholith. Precambrian Res 60:117–149

Bridgwater D, McGregor VR, Myers JS (1974) A horizontal tectonic regime in the Archaean of Greenland and its implications for early crustal thickening. Precambrian Res 1(3):179–197. https://doi.org/10.1016/0301-9268(74)90009-6

Bridgwater D, Mengel F, Fryer B, Wagner P, Hansen SC (1995) Early Proterozoic mafic dykes in the North Atlantic and Baltic cratons: field setting and chemistry of distinctive dyke swarms. Geol Soc Lond 95(1):193–210

Cadman AC, Tarney J, Bridgwater D, Mengel FC, Whitehouse M, Windley BF (2001) The petrogenesis of the Kangamiut dyke swarm, W Greenland. Precambrian Res 105:183–203

Champion DC, Smithies RH (2007) Geochemistry of Paleoarchean granites of the east Pilbara Terrane, Pilbara Craton, Western Australia: implications for early Archean crustal growth. In: Van Kranendonk MJ, Smithies RH, Bennett VC (eds) Earth's oldest rocks, vol 15. Elsevier, Amsterdam, pp 369–409

Dhuime B, Hawkesworth C, Cawood PA, Storey CD (2012) A change in the Geodynamics of continental growth 3 billion years ago. Science 335:1334–1336

Drummond MS, Defant MJ (1990) A model for Trondhjemite–Tonalite–Dacite Genesis and crustal growth via slab melting: Archean to modern comparisons. J Geophys Res 95(B13):21503. https://doi.org/10.1029/JB095iB13p21503

Fisher CM, Vervoort JD (2018) Using the magmatic record to constrain the growth of continental crust—the Eoarchean zircon Hf record of Greenland. Earth Planet Sci Lett 488:79–91. https://doi.org/10.1016/j.epsl.2018.01.031

Flowerdew MJ, Millar IL, Vaughan APM, Horstwood MSA, Fanning CM (2006) The source of granitic gneisses and migmatites in the Antarctic Peninsula: a combined U–Pb SHRIMP and laser ablation Hf isotope study of complex zircons. Contrib Miner Petrol 151:751–768

Foley S, Tiepolo M, Vannucci R (2002) Growth of early continental crust controlled by melting of amphibolite in subduction zones. Nature 417(6891):837–840. https://doi.org/10.1038/nature00799

Friend C, Nutman A (1994) Two Archaean granulite-facies metamorphic events in the Nuuk-Maniitsoq region, southern West Greenland: correlation with the Saglek block, Labrador. J Geol Soc 151:421–424

Friend C, Nutman A (2005) New pieces to the Archaean terrane jigsaw puzzle in the Nuuk region, southern West Greenland: steps in transforming a simple insight into a complex regional tectonothermal model. J Geol Soc 162:147–162

Friend C, Nutman A, McGregor VR (1987) Late-Archaean tectonics in the Færingehavn–Tre Brødre area, south of Buksefjorden, southern West Greenland. J Geol Soc 144(3):369–376

Friend C, Nutman A, McGregor VR (1988) Late Archaean terrane accretion in the Godthåb region, southern West Greenland. Nature 335:535–538

Friend C, Nutman A, Baadsgaard H, Kinny PD, McGregor VR (1996) Timing of late Archaean terrane assembly, crustal thickening and granite emplacement in the Nuuk region, southern West Greenland. Earth Planet Sci Lett 142:353–365

Friend CRL, Nutman AP, Baadsgaard H, Duke MJM (2009) The whole rock Sm–Nd 'age' for the 2825 Ma Ikkattoq gneisses (Greenland) is 800 Ma too young: Insights into Archaean TTG petrogenesis. Chem Geol 261(1–2):62–76. https://doi.org/10.1016/j.chemgeo.2008.09.019

Garde AA (1990) Thermal granulite-facies metamorphism with diffuse retrogression in Archaean orthogneisses, Fiskefjord, southern West Greenland. J Metamorph Geol 8:663–382

Garde AA (1997) Accretion and evolution of an Archaean high-grade grey gneiss—amphibolite complex: the Fiskefjord area, southern West Greenland. Geol Greenl Surv Bull 177:115

Garde AA (2007) A mid-Archaean island arc complex in the eastern Akia terrane, Godthåbsfjord, southern West Greenland. J Geol Soc 164:565–579

Garde AA, Larsen O, Nutman A (1986) Dating of late Archaean crustal mobilisation north of Qugssuk, Godthåbsfjord, southern West Greenland. Rapp Gronlands Geol Unders 128:25–36

Garde AA, Friend C, Nutman A, Marker M (2000) Rapid maturation and stabilisation of middle Archaean continental crust: the Akia terrane, southern West Greenland. Bull Geol Soc Den 47:1–27

Garde AA, McDonald I, Dyck B, Keulen N (2012a) Searching for giant, ancient impact structures on Earth: the Mesoarchaean Maniitsoq structure, West Greenland. Earth Planet Sci Lett 337–338:197–210. https://doi.org/10.1016/j.epsl.2012.04.026

Garde AA, Whitehouse M, Christensen R (2012b) Mesoarchean epithermal gold mineralization preserved at upper amphibolite-facies grade, Qussuk, southern West Greenland. Econ Geol 107:881–908

Garde AA, Dyck B, Esbensen KH, Johansson L, Möller C (2014) The Finnefjeld domain, Maniitsoq structure, West Greenland: differential rheological features and mechanical homogenisation in response to impacting? Precambrian Res 255:791–808. https://doi.org/10.1016/j.precamres.2014.06.022

Gardiner NJ, Hickman AH, Kirkland CL, Lu YJ, Johnson TE, Zhao JX (2017) Processes of crust formation in the early earth imaged through Hf isotopes from the East Pilbara Terrane. Precambrian Res 297:56–76. https://doi.org/10.1016/j.precamres.2017.05.004

Gardiner NJ, Johnson TE, Kirkland CL, Smithies RH (2018) Melting controls on the lutetium–hafnium evolution of Archaean crust. Precambrian Res 305:479–488. https://doi.org/10.1016/j.precamres.2017.12.026

Gardiner NJ, Johnson TE, Kirkland CL, Szilas K (2019) Modelling the Hafnium–Neodymium evolution of early earth: a study from West Greenland. J Petrol 60(1):177–197. https://doi.org/10.1093/petrology/egy110

Griffin W, Pearson NJ, Belousova E, Jackson SE, van Achterbergh E, O'Reilly SY, Shee SR (2000) The Hf isotope composition of cratonic mantle: LAM-MC-ICPMS analysis of zircon megacrysts in kimberlites. Geochim Cosmochim Acta 64(1):133–147

Hawkesworth CJ, Dhuime B, Pietranik AB, Cawood PA, Kemp AIS, Storey CD (2010) The generation and evolution of the continental crust. J Geol Soc 167(2):229–248. https://doi.org/10.1144/0016-76492009-072

Hawkesworth C, Cawood PA, Dhuime B, Kemp AI (2017) Earth's continental lithosphere through time. Annu Rev Earth Planet Sci 45:169–198. https://doi.org/10.1146/annurev-

Herzberg C, Condie K, Korenaga J (2010) Thermal history of the earth and its petrological expression. Earth Planet Sci Lett 292(1–2):79–88. https://doi.org/10.1016/j.epsl.2010.01.022

Hickman AH (1984) Archaean diapirism in the Pilbara Block, Western Australia. In: Kröner A, Greiling R (eds) Precambrian tectonics illustrated, vol E. Schweizerbarts'che Verlagsbuchhlung, Stuttgart, pp 113–127

Hiess J, Bennett VC, Nutman A, Williams IS (2011) Archaean fluid-assisted crustal cannibalism recorded by low d18O and negative eHf(T) isotopic signatures of West Greenland granite zircon. Contrib Miner Petrol 161:1027–1050. https://doi.org/10.1007/s00410-010-0578-z)

Hoffmann JE, Münker C, Næraa T, Rosing MT, Herwartz D, Garbe-Schönberg D, Svahnberg H (2011a) Mechanisms of Archean crust formation inferred from high-precision HFSE systematics in TTGs. Geochim Cosmochim Acta 75(15):4157–4178. https://doi.org/10.1016/j.gca.2011.04.027

Hoffmann JE, Münker C, Polat A, Rosing MT, Schulz T (2011b) The origin of decoupled Hf–Nd isotope compositions in Eoarchean rocks from southern West Greenland. Geochim Cosmochim Acta 75(21):6610–6628. https://doi.org/10.1016/j.gca.2011.08.018

Hoffmann JE, Nagel TJ, Münker C, Næraa T, Rosing MT (2014) Constraining the process of Eoarchean TTG formation in the Itsaq Gneiss Complex, southern West Greenland. Earth Planet Sci Lett 388:374–386. https://doi.org/10.1016/j.epsl.2013.11.050

Hoffmann JE, Kroner A, Hegner E, Viehmann S, Xie H, Iaccheri LM, Schneider KP, Hofmann AP, Wong J, Geng H, Yang J (2016) Source composition, fractional crystallization and magma mixing processes in the 3.48–3.43 Ga Tsawela tonalite suite (Ancient Gneiss Complex, Swaziland)—implications for Palaeoarchaean geodynamics. Precambrian Res 276:43–66

Johnson TE, Brown M, Kaus BJP, VanTongeren JA (2014) Delamination and recycling of Archaean crust caused by gravitational instabilities. Nat Geosci 7(1):47–52. https://doi.org/10.1038/ngeo2019

Johnson TE, Brown M, Gardiner NJ, Kirkland CL, Smithies RH (2017) Earth's first stable continents did not form by subduction. Nature 543:239–242. https://doi.org/10.1038/nature21383

Kalsbeek F, Garde AA (1989) Geological map of Greenland, 1: 500000, Frederikshåb Isblink–Søndre Strømfjord, sheet 2. Geological Survey of Denmark and Greenland, Copenhagen

Kamber BS (2015) The evolving nature of terrestrial crust from the Hadean, through the Archaean, into the Proterozoic. Precambrian Res 258:48–82. https://doi.org/10.1016/j.precamres.2014.12.007

Kamber BS, Collerson KD, Moorbath S, Whitehouse MJ (2003) Inheritance of early Archaean Pb-isotope variability from long-lived Hadean protocrust. Contrib Miner Petrol 145(1):25–46. https://doi.org/10.1007/s00410-002-0429-7

Kemp AIS, Wilde SA, Hawkesworth CJ, Coath CD, Nemchin A, Pidgeon RT, Vervoort JD, DuFrane SA (2010) Hadean crustal evolution revisited: new constraints from Pb–Hf isotope systematics of the Jack Hills zircons. Earth Planet Sci Lett 296(1–2):45–56. https://doi.org/10.1016/j.epsl.2010.04.043

Kirkland CL, Hollis J, Gardiner NJ (2016) Greenland U–Pb geochronology database. Nuuk. https://data.geus.dk/geusmap/?mapname=greenland_portal

Kirkland CL, Yakymchuk C, Hollis JA, Heide-Jorgensen H, Danišík M (2018a) Mesoarchean exhumation of the Akia terrane and a common Neoarchean tectonothermal history for West Greenland. Precambrian Res 314:129–144. https://doi.org/10.1016/j.precamres.2018.06.004

Kirkland CL, Yakymchuk C, Szilas K, Evans N, Hollis J, McDonald B, Gardiner NJ (2018b) Apatite: a U–Pb thermochronometer or geochronometer? Lithos 318–319:143–157. https://doi.org/10.1016/j.lithos.2018.08.007

Kroner A, Hoffmann JE, Xie H, Munker C, Hegner E, Wan Y, Hofmann AP, Liu D, Yang J (2014) Generation of early Archaean grey gneisses through melting of older crust in the eastern Kaapvaal craton, southern Africa. Precambrian Res 255:823–846. https://doi.org/10.1016/j.precamres.2014.07.017

Larsen LM, Rex DC (1992) A review of the 2500 Ma span of alkaline-ultramafic, potassic and carbonafitic magmatism in West Greenland. Lithos 28:367–402

Li X, Niu M, Yakymchuk C, Yan Z, Fu C, Zhao Q (2018) Anatexis of former arc magmatic rocks during oceanic subduction: a case study from the North Wulan gneiss complex. Gondwana Res 61:128–149

Marker M, Garde AA (1988) Border relations between the amphibolite facies Finnefjeld gneiss complex and granulite facies grey gneisses in the Fiskefjord area, southern West Greenland. Rapp Gronlands Geol Unders 140:49–54

Martin H (1986) Effect of steeper Archean geothermal gradient on geochemistry of subduction-zone magmas. Geology 14:753–756

McGregor VR, Friend C, Nutman A (1991) The late Archaean mobile belt through Godthåbsfjord, southern West Greenland: a continent–continent collision zone? Bull Geol Soc Den 39:179–197

Moorbath S, O'Nions RK, Pankhurst RJ, Gale NH, McGregor VR (1972) Further rubidium–strontium age determinations on the very early precambrian rocks of the Godthaab district, West Greenland. Nature 240:78–82. https://doi.org/10.1038/physci240078a0

Moyen J-F (2011) The composite Archaean grey gneisses: petrological significance, and evidence for a non-unique tectonic setting for Archaean crustal growth. Lithos 123(1–4):21–36. https://doi.org/10.1016/j.lithos.2010.09.015

Moyen J-F, Martin H (2012) Forty years of TTG research. Lithos 148:312–336. https://doi.org/10.1016/j.lithos.2012.06.010

Moyen JF, Stevens G (2006) Experimental constraints on TTG petrogenesis: implications for Archean geodynamics. In: Benn K, Mareschal J-C, Condie KC (eds) Archean geodynamics and environments: Geophysical monograph series, vol 164. American Geophysical Union, Washington DC, pp 149–178

Næraa T, Scherstén A (2008) New zircon ages from the Tasiusarsuaq terrane, southern West Greenland. Geol Surv Den Greenl Bull 15:73–76

Naeraa T, Schersten A, Rosing MT, Kemp AI, Hoffmann JE, Kokfelt TF, Whitehouse MJ (2012) Hafnium isotope evidence for a transition in the dynamics of continental growth 3.2 Gyr ago. Nature 485(7400):627–630. https://doi.org/10.1038/nature11140

Næraa T, Kemp AIS, Scherstén A, Rehnström EF, Rosing MT, Whitehouse MJ (2014) A lower crustal mafic source for the ca. 2550 Ma Qôrqut Granite Complex in southern West Greenland. Lithos 192–195:291–304. https://doi.org/10.1016/j.lithos.2014.02.013

Nutman A, McGregor VR, Friend CL, Bennett VC, Kinny PD (1996) The Itsaq Gneiss Complex of southern West Greenland; the world's most extensive record of early crustal evolution (3900–3600 Ma). Precambrian Res 78:1–39

Nutman A, Kalsbeek F, Marker M, van Gool JAM, Bridgwater D (1999) U–Pb zircon ages of Kangamiut dykes and detrital zircons in metasediments in the Palaeoproterozoic Nagssugtoqidian Orogen (West Greenland) clues to the pre-collisional history of the orogen. Precambrian Res 93:87–104

Nutman A, Christiansen O, Friend CRL (2007) 2635 Ma amphibolite facies gold mineralisation near a terrane boundary (suture?) on Storø, Nuuk region, southern West Greenland. Precambrian Res 159:19–32

Nutman AP, Bennett VC, Friend CRL, Yi K, Lee SR (2015) Mesoarchaean collision of Kapisilik terrane 3070 Ma juvenile arc rocks and> 3600 Ma Isukasia terrane continental crust (Greenland). Precambrian Res 258:146–160. https://doi.org/10.1016/j.precamres.2014.12.013

Palme H, O'Neill HSC (2003) Cosmochemical estimates of mantle composition. In: Carlson RW (ed) Treatise on geochemistry, vol 2. Elsevier, Oxford, pp 1–38

Rapp R (1991) Partial melting of amphibolite/eclogite and the origin of Archean trondhjemites and tonalites. Precambrian Res 51:1–25

Scherer EE, Munker C, Mezger K (2001) Calibration of the Lutetium–Hafnium Clock. Science 293:683–686

Scherstén A, Garde AA (2013) Complete hydrothermal re-equilibration of zircon in the Maniitsoq structure, West Greenland: a 3001 Ma minimum age of impact? Meteorit Planet Sci 48(8):1472–1498

Sizova E, Gerya T, Stüwe K, Brown M (2015) Generation of felsic crust in the Archean: a geodynamic modeling perspective. Precambrian Res 271:198–224. https://doi.org/10.1016/j.precamres.2015.10.005

Smithies RH, Van Kranendonk MJ, Champion DC (2007) The Mesoarchean emergence of modern-style subduction. Gondwana Res 11(1–2):50–68. https://doi.org/10.1016/j.gr.2006.02.001

Smithies RH, Champion DC, Van Kranendonk MJ (2009) Formation of Paleoarchean continental crust through infracrustal melting of enriched basalt. Earth Planet Sci Lett 281(3–4):298–306. https://doi.org/10.1016/j.epsl.2009.03.003

Steenfelt A, Garde AA, Moyen JF (2005) Mantle wedge involvement in the petrogenesis of Archaean grey gneisses in West Greenland. Lithos 79:207–228

Szilas K, van Gool JAM, Scherstén A, Frei R (2014) The Neoarchaean Storø supracrustal belt, Nuuk region, southern West Greenland: an arc-related basin with continent-derived sedimentation. Precambrian Res 247:208–222. https://doi.org/10.1016/j.precamres.2014.04.010

Szilas K, Kelemen PB, Bernstein S (2015) Peridotite enclaves hosted by Mesoarchaean TTG-suite orthogneisses in the Fiskefjord region of southern West Greenland. GeoResJ 7:22–34. https://doi.org/10.1016/j.grj.2015.03.003

Szilas K, Tusch J, Hoffmann JE, Garde AA, Münker C (2017) Hafnium isotope constraints on the origin of Mesoarchaean andesites in southern West Greenland, North Atlantic Craton. Geol Soc Lond 449(1):19–38. https://doi.org/10.1144/sp449.2

Tappe S, Pearson DG, Nowell G, Nielsen T, Milstead P, Muehlenbachs K (2011) A fresh isotopic look at Greenland kimberlites: cratonic mantle lithosphere imprint on deep source signal. Earth Planet Sci Lett 305(1–2):235–248. https://doi.org/10.1016/j.epsl.2011.03.005

Van Kranendonk MJ, Hugh Smithies R, Hickman AH, Champion DC (2007) Review: secular tectonic evolution of Archean continental crust: interplay between horizontal and vertical processes in the formation of the Pilbara Craton, Australia. Terra Nova 19(1):1–38. https://doi.org/10.1111/j.1365-3121.2006.00723.x

Windley BF, Garde AA (2009) Arc-generated blocks with crustal sections in the North Atlantic craton of West Greenland: crustal growth in the Archean with modern analogues. Earth Sci Rev 93(1–2):1–30. https://doi.org/10.1016/j.earscirev.2008.12.001

Winther KT, Newton RC (1991) Experimental melting of hydrous low-K tholeiite: evidence on the origin of Archean cratons. Bull Geol Soc Den 39:213–228

Yi K, Bennett VC, Nutman AP, Lee SR (2014) Tracing Archaean terranes under Greenland's Icecap: U–Th–Pb–Hf isotopic study of zircons from melt-water rivers in the Isua area. Precambrian Res 255:900–921. https://doi.org/10.1016/j.precamres.2014.04.006

Zeh A, Gerdes A, Barton JM (2009) Archean accretion and crustal evolution of the Kalahari Craton–the Zircon age and Hf isotope record of granitic rocks from Barberton/Swaziland to the Francistown Arc. J Petrol 50(5):933–966. https://doi.org/10.1093/petrology/egp027

Zeh A, Gerdes A, Millonig L (2011) Hafnium isotope record of the Ancient Gneiss Complex, Swaziland, southern Africa: evidence for Archaean crust–mantle formation and crust reworking between 3.66 and 2.73 Ga. J Geol Soc 168(4):953–964. https://doi.org/10.1144/0016-76492010-117